# Joint Iterative Equalization, Demapping, and Decoding with a Soft Interference Canceler

Markus A. Dangl, Werner G. Teich, Jürgen Lindner
University of Ulm, Dept. of Information Technology
Albert-Einstein-Allee 43, 89081 Ulm, Germany
{markus.dangl,werner.teich,juergen.lindner}@e-technik.uni-ulm.de

Jochem Egle
EADS Radio Communication Systems
Wörthstr. 85, 89077 Ulm, Germany
jochem.egle@eads.sysde.net

***Abstract*— High-level modulation alphabets offer an additional degree of freedom compared to the binary case, since several mappings from bits to symbols are possible. Recently, it was shown that using different mappings rather than Gray coding, a tremendous performance gain for AWGN channels can be obtained with iterative demapping and decoding. In this paper we include iterative demapping in a turbo equalization scheme and verify its improved performance over the conventional turbo scheme with the extrinsic information transfer (EXIT) chart tool.**

## I. Introduction

A coded transmission over a multipath channel disturbing the transmit symbols by intersymbol interference (ISI) may be interpreted as a serial concatenation of the code and the ISI channel. The optimum detection with respect to the bit error rate (BER) for this concatenation is in many cases prohibitively complex. Thus, often a sub-optimum approach is used where the received symbols are separately equalized and decoded. In particular, turbo equalization (joint equalization and decoding) represents a well-known sub-optimum technique, where both equalizer and decoder benefit from each other during an iterative process [1], [2].

In this paper we consider a turbo equalization scheme that consists of the optimum symbol-by-symbol APP decoder (BCJR algorithm [3]) and a soft interference canceler as equalizer. This soft interference canceler has the structure of a recurrent neural network (RNN). Hence, we term this equalizer RNN in the following. It was introduced in, e. g. , [4] and [5]. In [6] a comparison of different variants of the RNN in the context of multiuser detection is presented. An extension of the equalizer to a coded transmission and higher modulation alphabets can be found in, e. g. , [7] and [8].

Iterative demapping and decoding (IDEM) has shown to be advantageous in the context of $M$-ary symbol alphabets [9], [10], and [11]. In the case of AWGN channels this scheme closely approaches the capacity limit when combined with proper mapping from bits to symbols. We show that iterative demapping can also be used to improve the BER performance in the case of ISI channels, where additionally an equalizer is required. The convergence of the proposed turbo scheme is visualized using the extrinsic information transfer (EXIT) chart tool [11].

In Section II we introduce the system model. Then, in Section III we describe both conventional turbo equalization and the new turbo scheme (joint equalization, demapping, and decoding). We give a brief introduction to EXIT charts and present a simple algorithm for constructing mappings for AWGN channels in Section IV. Simulation results for ISI channels are shown in Section V. Finally, Section VI summarizes essential results.

## II. System Model

Fig. 1 shows the transmission model. A sequence of bits $\underline{q}$

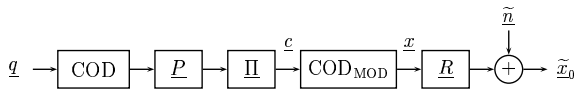


Fig. 1. Transmission model.

is encoded with a terminated convolutional code, optionally punctured with the puncturing matrix $\underline{P}$ and permuted by a random interleaver $\underline{\Pi}$. The code sequence $\underline{c}$ is mapped to the symbols of an $M$-ary symbol alphabet $\mathcal{A}_x = \{a_1, \ldots, a_M\}$ that can be complex-valued. These symbols $\underline{x}$ are transmitted over a linear time-invariant multipath channel. The receive side consists of a filter that is matched to both the transmit pulse and channel impulse response (CIR). We insert a guard time between blocks of $N_B$ symbols to avoid interblock interference. Hence, we obtain a block of $N_B$ received symbols $\underline{\widetilde{x}}_0$ using a discrete-time vector-valued model on symbol-basis [12]:

$$\underline{\widetilde{x}}_0 = \underline{R}\,\underline{x} + \underline{\widetilde{n}}, \tag{1}$$

where $\underline{R}$ denotes the $N_B \times N_B$ autocorrelation matrix of the convolution of the transmit pulse with the CIR, and $\underline{\widetilde{n}}$ is a vector of colored noise samples with covariance matrix $2\,N_0\,\underline{R}$ for complex-valued or $N_0\,\underline{R}$ for real-valued alphabets, respectively. The component variances of the complex AWGN process before the channel matched filter are $\sigma_n^2 = N_0$.

## III. Joint Equalization, Demapping, and Decoding

First we describe conventional joint equalization and decoding. Then, we proceed with the new scheme of joint equalization, demapping, and decoding.

### A. Joint Equalization and Decoding with an RNN

Fig. 2 depicts the receiver structure for joint equalization and decoding with an RNN equalizer. It was introduced for parallel interference cancellation in [7] and is described for the serial case in [13]. Within one iteration the received vector $\underline{\widetilde{x}}_0$ is first processed by the RNN equalizer and then by the decoder. The output of the equalizer are soft values which are fed to the decoder after deinterleaving ($\underline{\Pi}^{-1}$) and depuncturing ("$\underline{P}^{-1}$"). Then, the extrinsic soft values of the decoder are punctured, interleaved, and provided to the equalizer.

First we consider the equalization step in more detail. Let us focus on the $i$th symbol. Fig. 3 shows the calculation of

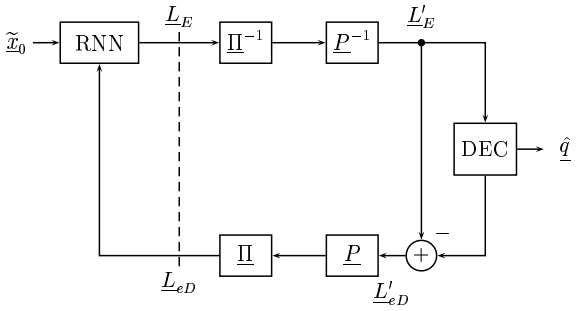


Fig. 2. Joint equalization and decoding with an RNN.

the partially equalized symbol $\widetilde{x}_i^{[l]}$ and new soft estimate $\breve{x}_i^{[l]}$ of the $i$th symbol in the $l$th iteration ($i = 1, \ldots, N_B$). We

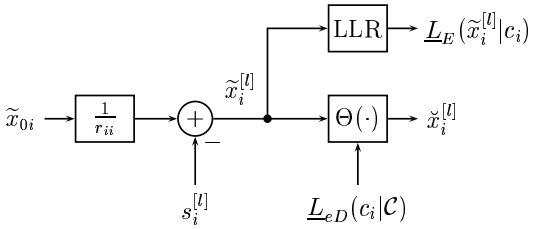


Fig. 3. Update of symbol $\breve{x}_i$.

subtract the estimated interference $s_i^{[l]}$ originating from all other symbols in the block from the scaled received symbol:

$$\begin{aligned}\widetilde{x}_i^{[l]} &= \widetilde{x}_{0i}/r_{ii} - s_i^{[l]} \\ &= \widetilde{x}_{0i}/r_{ii} - \left(\sum_{j=1}^{i-1} \frac{r_{ij}}{r_{ii}}\, \breve{x}_j^{[l]} + \sum_{j=i+1}^{N_B} \frac{r_{ij}}{r_{ii}}\, \breve{x}_j^{[l-1]}\right), \quad (2)\end{aligned}$$

where $r_{ij}$ denotes the element of $i$th row and $j$th column of $\underline{R}$. We refer to (2) as *serial update*, since besides soft estimates from the previous iteration $l-1$ also estimates from the current iteration $l$ are considered. The calculation of the soft estimates (feedback) is according to [14], [15], where we interpret the code $\mathcal{C}$ as an additional condition:

$$\breve{x}_i^{[l]} = \Theta(\widetilde{x}_i^{[l]}) = \mathrm{E}\{x_i|\widetilde{x}_i^{[l]}, \mathcal{C}\} = \sum_{j=1}^{M} a_j\, P(x_i = a_j|\widetilde{x}_i^{[l]}, \mathcal{C}). \quad (3)$$

Applying Bayes' rule and assuming statistical independence between the two conditions $\mathcal{C}$ and $\widetilde{x}_i^{[l]}$ we obtain:

$$P(x_i = a_j|\widetilde{x}_i^{[l]}, \mathcal{C}) = \frac{p(\widetilde{x}_i^{[l]}|x_i = a_j)\, P(x_i = a_j|\mathcal{C})}{p(\widetilde{x}_i^{[l]})}. \quad (4)$$

The statistical independence is justified by the use of the random interleaver and holds at least in the first iteration. We obtain the probability $P(x_i = a_j|\mathcal{C})$ in (4) by using the extrinsic information of the decoder. The vector $\underline{L}_{eD}(c_i|\mathcal{C})$ contains the $\log_2 M$ extrinsic $L$-values $L_{eD}(c_{i,\nu}|\mathcal{C})$ ($\nu = 1, \ldots, \log_2 M$) of the $i$th symbol. The $L$-value of a bit $c$ is defined by its probabilities: $L(c) = \ln \frac{P(c=0)}{P(c=1)}$. Thus, we get for $P(x_i = a_j|\mathcal{C})$:

$$P(x_i = a_j|\mathcal{C}) = \prod_{\nu=1}^{\log_2 M} \frac{\exp\big((1 - \mathrm{bin}[a_j, \nu])L_{eD}(c_{i,\nu}|\mathcal{C})\big)}{1 + \exp\big(L_{eD}(c_{i,\nu}|\mathcal{C})\big)}, \quad (5)$$

where $\mathrm{bin}[a_j, \nu]$ denotes the value of the $\nu$th bit of the bit vector mapped to the symbol $a_j$. The block LLR (log-likelihood ratio) in Fig. 3 evaluates the channel reliability values $L_E(\widetilde{x}_i^{[l]}|c_{i,\nu})$ of the code bits ($\nu = 1, \ldots, \log_2 M$):

$$L_E(\widetilde{x}_i^{[l]}|c_{i,\nu}) = \ln \frac{\sum_{a_j \in \mathcal{A}_\nu^{[0]}} p(\widetilde{x}_i^{[l]}|x_i = a_j)}{\sum_{a_j \in \mathcal{A}_\nu^{[1]}} p(\widetilde{x}_i^{[l]}|x_i = a_j)}, \quad (6)$$

where $\mathcal{A}_\nu^{[b]}$ denotes a subset of $\mathcal{A}_x$ that contains all symbols with the $\nu$th bit being equal to $b$ ($b = 0, 1$). The probability densities $p(\widetilde{x}_i^{[l]}|x_i = a_j)$ are assumed to be Gaussian [14].

The input $L$-values $\underline{L}'_E$ of the decoder are subtracted from the output values to obtain extrinsic information $\underline{L}'_{eD}$ which is used for the next iteration.

### B. Joint Equalization, Demapping, and Decoding with an RNN

We omit a detailed description of iterative demapping and focus on the basic principle only. For more information the reader may refer to, e. g., [9]. The calculation of the channel $L$-values (demapping) in (6) assumes that we have no a priori knowledge about the bits. However, the extrinsic information of the decoder can be treated as a priori knowledge of the code bits for the demapper (LLR block in Fig. 3). In [9] an iterative scheme is proposed that consists of a demapper and a decoder. It is shown that the demapper benefits from the additional information coming from the decoder. If we have no a priori knowledge about the code bits Gray mapping performs best. However, through the iterative process we gain a priori information that is more useful for non-Gray mappings, since neighboring symbols in the signal constellation might differ in more than only one bit.

Fig. 4 shows the modified calculation of the $L$-values. In contrast to the detector depicted in Fig. 3, the extrinsic information of the code is now exploited for both the soft decision function $\Theta(\cdot)$ and the calculation of the $L$-values.

$$L_E^a(\widetilde{x}_i^{[l]}|c_{i,\nu}) = \ln \frac{\sum\limits_{a_j \in \mathcal{A}_\nu^{[0]}} p(\widetilde{x}_i^{[l]}|x_i = a_j) \prod\limits_{k \neq \nu} \exp\big((1 - \mathrm{bin}[a_j, k]) L_{eD}(c_{i,k}|\mathcal{C})\big)}{\sum\limits_{a_j \in \mathcal{A}_\nu^{[1]}} p(\widetilde{x}_i^{[l]}|x_i = a_j) \prod\limits_{k \neq \nu} \exp\big((1 - \mathrm{bin}[a_j, k]) L_{eD}(c_{i,k}|\mathcal{C})\big)}. \tag{7}$$

We subtract the a priori $L$-values from the a posteriori $L$-values [9] and obtain the channel and extrinsic $L$-values of the demapper $L_E^a(\widetilde{x}_i^{[l]}|c_{i,\nu})$ according to (7). (7) can be derived using Bayes' rule, (5), and (6). The superscript $^a$ indicates

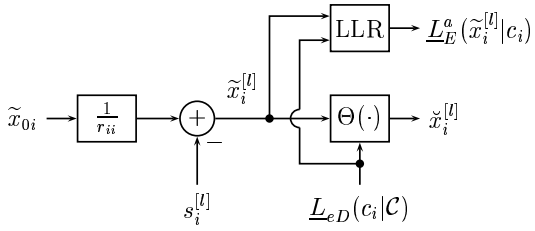


Fig. 4. Modified calculation of LLR.

that the demapper takes a priori information of the bits into account. Consequently, we replace in Fig. 2 $\underline{L}_E$ by $\underline{L}_E^a$ and $\underline{L}_E'$ by $\underline{L}_E^{a\,\prime}$, respectively. We refer to this modified new scheme as joint iterative equalization, demapping and decoding with the RNN.

## IV. EXIT Curves

Convergence behavior of iterative decoding schemes can be visualized by means of mutual information between transmitted bits and $L$-values in the turbo scheme. A comprehensive overview of this method for iterative demapping, turbo equalization, and turbo decoding can be found in [11].

First we describe the basic principles of the EXIT chart tool and then discuss demapper characteristics of the symbol alphabets that are later used in Section V. Furthermore, we present a simple algorithm for constructing mappings.

### A. EXIT Chart

Let us focus on the decoder. We assume perfect interleaving. Therefore, the input $L$-values of the decoder can be modeled by independent and identically distributed random variables. The probability density function (pdf) of these random variables $A_D$ conditioned on the transmitted code bits $W$ is Gaussian with mean $\sigma_A^2/2 \cdot (1 - 2\,c)$ (with $c = 0, 1$) and variance $\sigma_A^2$. The information content $I_{\mathrm{A,Dec}} := I(W; A_D)$ between $W$ and $A_D$ depends on $\sigma_A$ by a one-to-one relationship. It can be evaluated numerically [11]. Similarly, the mutual information $I_{\mathrm{E,Dec}} := I(W; E_D)$ between $W$ and the extrinsic decoder output random variables $E_D$ can be determined by observing the pdf of $E_D$. The mutual output information $I_{\mathrm{E,Dec}}$ as a function of the mutual input information $I_{\mathrm{A,Dec}}$ is denoted as the *extrinsic transfer characteristics* of the decoder.

The extrinsic transfer characteristics of the demapper and of memoryless equalizers might be obtained with the procedure described above. However, in the case of the RNN equalizer we observe that the output $L$-values depend with (2) on the symbol estimates $\breve{\underline{x}}$ of both the current and the previous iteration. This memory can be reproduced by running the RNN equalizer with more than one iteration and using the same extrinsic information in each iteration [13]. The feedback vector $\breve{\underline{x}}$ is initialized to zero for the first iteration. Thus, the extrinsic information of the decoder is used first for the second symbol in the first iteration according to (2). We note that this approach only approximately describes the transfer characteristics of the RNN equalizer. However, for simplicity we apply the method described above in Section V. The plots of both transfer characteristics (decoder and equalizer/demapper) together with the true trajectory of the iterative decoding scheme build the EXIT chart. The dashed vertical line in Fig. 2 indicates where the pdf of the $L$-values is determined.

### B. Demapper Transfer Characteristics

Tables I and II show mappings for $4$ ASK and $8$ QAM we want to focus on in the sequel. For $4$ ASK there are only three significantly different mappings [9], whereas in the case of $8$ QAM much more exist. Among these we chose two interesting examples, mapping M1 and M2. The

TABLE I
MAPPINGS FOR 4 ASK.

| symbols | $-3$ | $-1$ | $1$ | $3$ |
|---|---|---|---|---|
| Gray | 00 | 10 | 11 | 01 |
| natural | 00 | 01 | 10 | 11 |
| anti Gray | 00 | 11 | 10 | 01 |

mutual input and output information of the demapper shall be denoted as $I_{\mathrm{A,Dem}}$ and $I_{\mathrm{E,Dem}}$, respectively. Similarly, we define $I_{\mathrm{A,EQ}}$ and $I_{\mathrm{E,EQ}}$ for the equalizer. Figs. 5 and 6 show the demapper characteristics of the specified mappings for $4$ ASK and $8$ QAM. Additionally, both graphs contain the decoder characteristics of a memory 2, rate $\frac{1}{2}$ code with generator polynomials $[7\ \ 5]_8$ (CC(7,5)). The values of the demapper characteristics with no a priori knowledge and full a priori knowledge shall be denoted by $I_0$ and $I_1$, respectively. Fig. 5 illustrates that anti Gray mapping performs best as long as the demapper characteristics lies above the decoder characteristics. The crucial observation of ten Brink [9] was that such a mapping with good BER performance in iterative decoding schemes, i. e., large $I_1$, is usually connected to small $I_0$. Therefore, a "good" mapping offers a large $I_1$ while still allowing convergence. Fig. 6 depicts the transfer

TABLE II
MAPPINGS FOR 8 QAM.

| symbols | $1+\mathrm{j}$ | $-1+\mathrm{j}$ | $-1-\mathrm{j}$ | $1-\mathrm{j}$ | $1+\sqrt{3}$ | $(1+\sqrt{3})\mathrm{j}$ | $-1-\sqrt{3}$ | $(-1-\sqrt{3})\mathrm{j}$ |
|---|---|---|---|---|---|---|---|---|
| M1 | 100 | 111 | 001 | 010 | 000 | 110 | 101 | 011 |
| M2 | 110 | 101 | 001 | 111 | 000 | 011 | 010 | 100 |

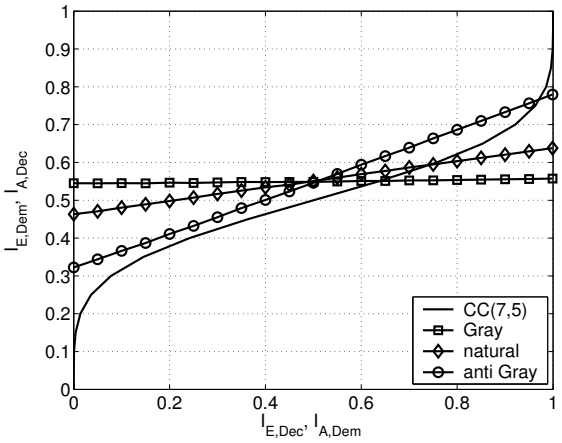


Fig. 5. Demapper characteristics for 4 ASK at $E_b/N_0 = 6$dB.

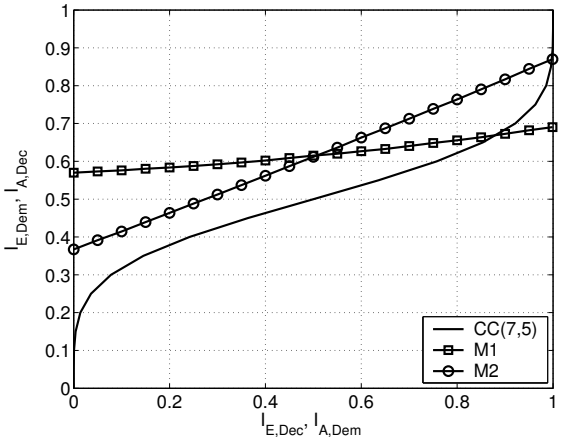


Fig. 6. Demapper characteristics for 8 QAM at $E_b/N_0 = 6$dB.

characteristics with largest $I_0$ (M1) and largest $I_1$ (M2) for 8 QAM; Gray mapping does not exist for this QAM alphabet.

Note that $I_0$ and $I_1$ can be approximately calculated for AWGN channels [11]. Furthermore, the area $\mathcal{F}$ under the demapper characteristics corresponds to the channel capacity under certain conditions [16]. Thus, since the demapper transfer curves for the chosen examples are almost straight lines, we obtain the following approximate relationship:

$$C(\mathcal{A}_x)/\log_2 M \approx \mathcal{F} \approx (I_0 + I_1)/2, \tag{8}$$

where $C(\mathcal{A}_x)$ denotes the channel capacity when using the symbol alphabet $\mathcal{A}_x$ with identical prior probabilities of the symbols.

Adequate mappings could be found by applying an exhaustive search which might be in some cases too complex. A simple algorithm for a construction of "moderate" mappings that could be used for AWGN channels is explained in the following. It is based on the idea that we start with Gray mapping or a mapping that is close to Gray like M1. By exchanging the bit labels of neighboring symbols we gradually decrease $I_0$ that has to be larger than a certain minimum value $I_{0,\min}$. Furthermore, the ordered set $\mathcal{S}$ shall contain all symbols of $\mathcal{A}_x$ such that neighboring symbols in the signal space are also neighbors or lie at least close together in $\mathcal{S}$. Each position in $\mathcal{S}$ corresponds to a specific bit label. Algorithm:

```
input:
ordered set S, minimum required I_0,min
initialization:
S_best := S and I_0,best := I_0(S)
for i:=1:M-1
   swap ith and (i+1)th symbol in S
   calculate I_0(S)
   if I_0<I_0,best and I_0>I_0,min then
     I_0,best := I_0, S_best := S
   end
end
output: S_best, I_0,best
```

Note that the corresponding $I_{1,\mathrm{best}}$ can be calculated as described in [11] or approximated via (8). In the case of 8 QAM, $E_b/N_0 = 6$dB, and $I_{0,\min} = 0.4$ we obtain a mapping with $I_{0,\mathrm{best}} \approx 0.50$ and $I_{1,\mathrm{best}} \approx 0.73$ that lies in between the corresponding points of M1 and M2 as expected (Fig. 6). The application of this algorithm for ISI channels might be possible by modelling the interference as additional Gaussian noise. However, since in these cases the quality of the output of the algorithm, i. e., the match of the predicted $I_0$ to the true $I_0$, depends strongly on the type of ISI channel, we omit results, here.

$I_1$ does not change for the ISI channel and an RNN equalizer compared to the AWGN channel, since the ISI can be perfectly removed with perfect a priori knowledge, but $I_0$ becomes smaller. Therefore, the mapping has to be chosen even more carefully than for AWGN channels. In the following we show simulation results for iterative demapping in the presence of ISI.

## V. SIMULATION RESULTS

We choose for the CIR (taps are T-spaced) two examples: channel (a) with $\underline{h} = 1/\sqrt{2}\,[1\ 1]^T$ and channel (b) with

$\underline{h} = [0.407\ 0.815\ 0.407]^T$ from [17]. The convolutional code is rate $\frac{1}{2}$ with memory 2 and generator polynomials $[7\ 5]_8$. A block of 10000 information bits is encoded to 20004 code bits. The interleaver size is also 20004. Thus, one block has $N_B = 10002$ symbols for 4 ASK and $N_B = 6668$ symbols for 8 QAM. The number of iterations in the joint equalization and decoding scheme (RNN) and for joint equalization, demapping, and decoding (RNN+IDEM) is 15 as well as for the AWGN reference curves. Fig. 7 shows the BER for 4 ASK and channel (a). As references the Shannon limit of

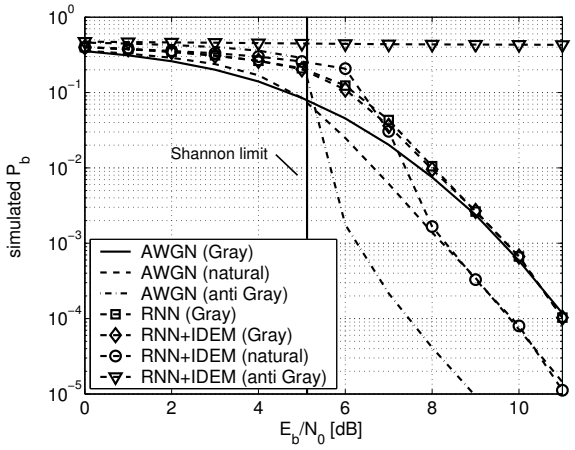


Fig. 7. BER for 4 ASK and channel (a).

the AWGN channel (vertical line) and AWGN performance of the mappings is included. As expected there is almost no difference between RNN and RNN+IDEM when using Gray mapping. However, natural mapping is advantageous at $E_b/N_0$ beyond 7dB and outperforms Gray mapping despite ISI. Unfortunately, anti Gray mapping does not converge at all for this channel. This behavior can be verified by the EXIT curves shown in Fig. 8. The trajectory of the

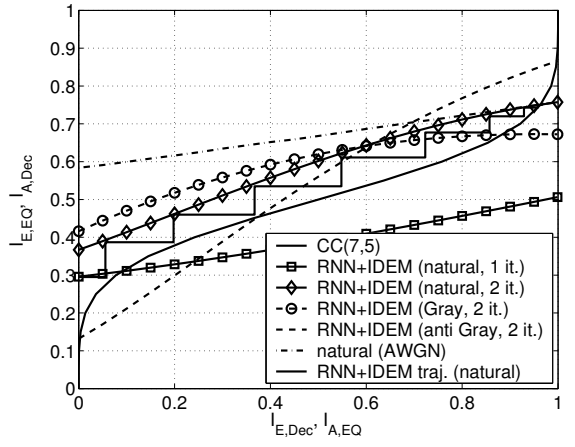


Fig. 8. EXIT chart for 4 ASK and channel (a) at $E_b/N_0 = 8$dB.

RNN+IDEM scheme with natural mapping is in between the decoder characteristics and the RNN+IDEM characteristics using 1 (squares) and 2 iterations (diamonds), respectively [13]. The curve with Gray mapping (circles) starts at higher $I_0$ and therefore Gray mapping performs better than natural mapping in the case of low a priori information. On the other hand, the intersection with the decoder transfer function is at lower output information. Thus, the BER performance for high a priori information is worse than using natural mapping. Additionally, the plot shows that the RNN+IDEM curve (diamonds) converges to the AWGN demapper curve (dashed dotted line) for perfect a priori knowledge. The curve for anti Gray mapping (dashed line) starts below the decoder characteristics so that reasonable BER performance cannot be achieved for the chosen code and equalizer.

Figs. 9 and 10 show similar results for 8 QAM and channel (b). Since the equalizer for mapping M2 does not converge to

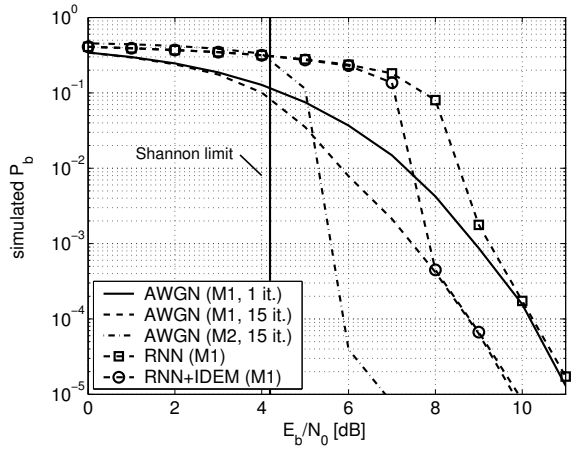


Fig. 9. BER for 8 QAM and channel (b), M1 and M2 see Table II.

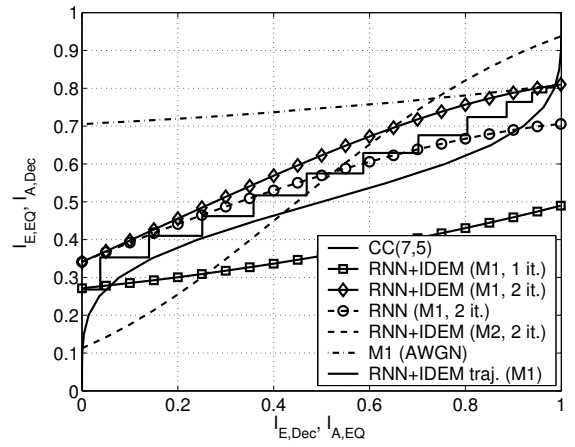


Fig. 10. EXIT chart for 8 QAM and channel (b) at $E_b/N_0 = 8$dB.

low BER like in the previous example for anti Gray mapping, we omit the corresponding curve. As the figure illustrates we see that it is useful to apply iterative demapping for the M1 mapping *in any case*, since the potential for a performance gain is inherently given and M1 offers the largest $I_0$. In the ISI case the complexity for iterative demapping (RNN+IDEM) increases only little due to the more complex formula (7), but

the effort in terms of decoding steps is not higher than for the joint decoding scheme without demapping (RNN).

## VI. Conclusions

We derived a new soft iterative interference cancellation scheme (RNN+IDEM) that exploits extrinsic demapper transfer characteristics. Its performance gain over the conventional scheme (RNN) was verified with the EXIT chart tool. Furthermore, simulation results showed that in some cases AWGN performance can be achieved even for non-Gray mappings. A simple algorithm for the construction of moderate mappings in AWGN environment was introduced. Iterative demapping and decoding leads also to an improved performance when suitably combined with other types of equalizers like the Soft Cholesky Block Decision Feedback Equalizer [14], which was shown in the context of multi-carrier MIMO systems in [18]. Future work will include the use of more sophisticated channel codes and the assumption of imperfect channel state information. This paper is published in [19].

## Acknowledgment

The authors would like to thank Christian Sgraja for his helpful comments, and gratefully acknowledge the support by the COST 289 Action.

## References

[1] C. Douillard, M. Jezequel, C. Berrou, A. Picart, P. Didier, and A. Glavieux, "Iterative correction of intersymbol interference: Turbo-equalization," *European Trans. Telecomm.*, vol. 6, no. 5, pp. 507–511, Sept./Oct. 1995.

[2] M. Tüchler, R. Koetter, and A. Singer, "Turbo equalization: Principles and new results," *IEEE Trans. Commun.*, vol. 50, no. 5, pp. 754–767, May 2002.

[3] L. R. Bahl, J. Cocke, F. Jelinek, and J. Raviv, "Optimal decoding of linear codes for minimizing symbol error rate," *IEEE Trans. Inform. Theory*, vol. 20, pp. 284–287, Mar. 1974.

[4] W. G. Teich and M. Seidl, "Code division multiple access communications: Multiuser detection based on a recurrent neural network structure," in *Proc. IEEE ISSSTA*, vol. 3, Mainz/Germany, Sept. 1996, pp. 979–984.

[5] R. R. Müller and J. B. Huber, "Iterated soft-decision interference cancellation for CDMA," in *Proc. 9th Int. Tyrrhenian Workshop on Digital Communications*, Lerici/Italy, Sept. 1997.

[6] A. Engelhart, W. G. Teich, J. Lindner, G. Jeney, S. Imre, and L. Pap, "A survey of multiuser/multisubchannel detection schemes based on recurrent neural networks," *Wireless Communications and Mobile Computing*, vol. 2, no. 3, pp. 269–284, May 2002.

[7] C. Sgraja, A. Engelhart, W. G. Teich, and J. Lindner, "Combined equalization and decoding for BFDM packet transmission schemes," in *Proc. 1st Int. OFDM-Workshop*, Hamburg/Germany, Sept. 1999, pp. 19–1ff.

[8] ——, "Multiuser/multisubchannel detection based on recurrent neural network structures for linear modulation schemes with general complex-valued symbol alphabet," in *Proc. COST 262 Workshop on Multiuser Detection in Spread Spectrum Communications*, Reisensburg/Germany, Jan. 2001, pp. 45–52.

[9] S. ten Brink, J. Speidel, and R. Yan, "Iterative demapping and decoding for multilevel modulation," in *Proc. IEEE GLOBECOM*, Sydney/Australia, Nov. 1998, pp. 579–584.

[10] S. ten Brink, J. Speidel, and R.-H. Han, "Iterative demapping for QPSK modulation," *Electronics Letters*, vol. 34, no. 15, pp. 1459–1460, July 1998.

[11] S. ten Brink, "Designing iterative decoding schemes with the extrinsic information transfer chart," *AEÜ Int. Jour. Electron. Commun.*, vol. 54, no. 6, pp. 389–398, Nov. 2000.

[12] J. Lindner, "MC-CDMA in the context of general multiuser/multisubchannel transmission methods," *European Trans. Telecomm.*, vol. 10, no. 5, pp. 351–367, July/Aug. 1999.

[13] M. A. Dangl, C. Sgraja, W. G. Teich, J. Lindner, and J. Egle, "Convergence behavior of iterative equalization and decoding schemes with memory," in *Proc. IEEE GLOBECOM*, San Francisco/US, Dec. 2003, accepted for publication.

[14] J. Egle and J. Lindner, "Iterative joint equalization and decoding based on soft cholesky equalization for general complex valued modulation symbols," in *Proc. 6th Int. Symposium on DSP for Communication Systems*, Sydney-Manly/Australia, Jan. 2002, pp. 163–170.

[15] J. Egle, "Detection of power and bandwidth efficient single carrier block transmission," Ph.D. dissertation, University of Ulm, Department of Information Technology, 2003, to appear.

[16] A. Ashikhmin, G. Kramer, and S. ten Brink, "Extrinsic information transfer functions: a model and two properties," in *Proc. CISS*, Princeton/US, Mar. 2002.

[17] J. G. Proakis, *Digital Communications*, 3rd ed. McGraw-Hill, 1998.

[18] M. A. Dangl, D. Yacoub, U. Marxmeier, W. G. Teich, and J. Lindner, "Performance of joint detection techniques for coded MIMO-OFDM and MIMO-MC-CDM," in *Proc. COST 273 Workshop on Broadband Wireless Local Access*, Paris/France, May 2003, pp. 17/1–17/6.

[19] M. A. Dangl, W. G. Teich, J. Lindner, and J. Egle, "Joint iterative equalization, demapping, and decoding with a soft interference canceler," in *Proc. Int. Symp. on Commun. Theory and Appl.*, Ambleside/UK, July 2003, accepted for publication.